*Korean J. Chem. Eng.*, 32(10), 1986-1992 (2015)
DOI: 10.1007/s11814-015-0041-y

pISSN: 0256-1115
eISSN: 1975-7220

# Efficient sorption and photocatalytic degradation of malachite green dye onto NiS nanoparticles prepared using novel green approach

**Kumar Suranjit Prasad*,†, Sheel Prajapati**, and Kaliaperumal Selvaraj*****

*Department of Environmental Studies, Faculty of Science, The M. S. University of Baroda, 390002, Vadodara, Gujarat, India
**Department of Environmental Sciences, Ashok & Rita Patel Institute of Integrated Study & Research in Biotechnology and Allied Sciences (ARIBAS), New Vallabh Vidyanagar, Anand, Gujarat, 388121, India
***Nano and Computational Materials Lab, Catalysis Division, National Chemical Laboratory, Council of Scientific and Industrial Research, Pune - 411008, India
(*Received 4 June 2014 • accepted 25 February 2015*)

**Abstract**−The extract of the *Asparagus racemosus* leaf tissue works as a stabilizing and capping agent and assists the formation of stable colloidal nanoparticles. Nanoparticles were characterized using UV-vis spectrophotometer, photoluminescence, TEM, EDAX and XRD, respectively. Transmission electron microscopy followed by selected area electron diffraction pattern analysis indicated the formation of near spherical, polydispersed, crystalline NiS of diameter ranging from 4-27 nm. X-ray diffraction studies showed the formation of 110, 101, 300, 021, 220, 221, 131, 410, 401, 321, 330 and 021 planes of hexagonal NiS. EDAX analysis confirmed the presence of Ni and S in nanosphere. The maximum sorption capacity ($q_m$) of NiS nanoparticles for MG dye was found to be 64.85 mg/g. Decolorization as well as disintegration of malachite green under white light illumination was confirmed by LC-MS studies. Results of the present study suggest that nanosized NiS can play an instrumental role in photocatalytic degradation of malachite green dye present in water bodies.

Keywords: NiS Nanoparticles, Malachite Green, Degradation, TEM, FTIR

## INTRODUCTION

Dyes are designed to be chemically and photolytically stable, hence they are highly persistent in natural environments. The synthetic azo dyes consisting of aromatic rings are inert and non-biodegradable [1] and have been considered as carcinogenic as they harbor azo bonds nitro- or amino-groups [2,3]. Approximately 70% of the dyes are aromatic azo compounds [4,5] with application in the textile industry, leather tanning, paper production, food technology, agricultural research [6] light-harvesting arrays, photoelectrochemical cells and hair color production [8]. The textile trade accounts for two-thirds of the total dyestuff arcade, and during the dyeing process approximately 10% of the dyes used are discharged into the waste-water. Besides toxicity, wastewaters containing dye from textile industries have high TOC, high salt content and extreme pH [8]. Malachite green (MG) belongs to triphenylmethane dyes, which are widely used in textile as well as fish farming industry. It possesses microbicidal property against fish pathogen and remains popular among fish farmers due to low cost factor. MG is considered to be toxic to mammalian cells and their usage is banned by the US Food and Drug Administration [9]. There is concern about the fate of MG and its reduced form, leucomalachite green, in aquatic and terrestrial ecosystems since they occur as contaminants [10].

†To whom correspondence should be addressed.
E-mail: suranjit@gmail.com


A wide range of approaches including physical and chemical methods like coagulation, adsorption, flocculation, precipitation, irradiation, membrane filtration, ozonization, Fenton's oxidation, decolorization by photocatalysis or by oxidation processes, microbiological or enzymatic decomposition have been used in degradation of dyes present in water bodies [6]. Sulfide semiconductor possessing wide band gap has been considered as an excellent photocatalyst in visible light region [11]. NiS nanoparticles (NPs) band gap is of order of 3.63 eV, while bulk NiS is 0.4 eV, which makes them superior semiconductors [13,14]. Recent regulatory pressure to decrease or eradicate the use of lead and cadmium has prompted investigators to search for alternative materials. NiS NPs reduced the level of chloride, fluoride, nitrate, calcium, magnesium, iron, cadmium contents and total hardness of raw water [14]. The efficient adsorption of congo red by hydrothermally synthesized NiS NPs has been studied [15]. A comparison of the photoefficiency of Ni(II) and NiS incorporated into zeolite P towards photodecolorization of Eriochrome Black T dye solution was investigated in a photocatalytic reactor using UV lamp as a light source [16]. NiS-P zeolite prepared by ion exchange and precipitation procedures has been used as a catalyst for photodecolorization of Eriochrome Black T under UV irradiation [17]. Co-precipitated NiS-ZnS exhibits higher photocatalytic activity than pure ZnS [18]. Reductive degradation of an orange G azo dye, using Fe-Ni bimetallic nanoparticles in aqueous solution, has been reported by Bokare et al. [19]. ZnO, $TiO_2$ and Ag/ZnO nanoparticles have been examined as photocatalysts for degradation of azo dyes, such as methyl red, methyl

orange [20,21] and methylene blue [22] in water. The degradation efficiency largely depends on the adsorption behavior of photocatalyst and pollutant molecules. [23,24]. Certain established methods for nanoparticles synthesis are precipitation, electrochemical deposition, sputtering [25] inverse micelles, sonochemical, microwave assisted and recently via green chemistry route [26] vapor deposition, mechanical ball milling, molecular beam epitaxy [27] reduction in aqueous solution with or without stabilizing agent [28] photo-reduction and radiation-assisted synthesis [29]. Scientists across the globe have shown keen interest in the potential of various herbs, algae, fungi, bacteria and viruses for synthesis of metallic nanoparticles [30]. Biomolecules such as enzymes/proteins, polysaccharides and secondary metabolites in the extract act as a capping and reducing agent and are chiefly accountable for the stability [31,32]. In this present study, synthesis and characterization of NiS nanoparticles using leaf extract of *Asparagus racemosus* was carried out. The study further explores the utility of these nanoparticles in degradation of malachite green azo dye under white light exposure.

## EXPERIMENTAL

### 1. Synthesis of NiS Nanoparticles and Photoluminescence Study

Leaves (5 g) of *Asparagus racemosus* plant were macerated in 20 ml of Tris.Cl (20 mM, pH 7.5). Thick slurry of leaf was subjected to centrifugation at 10,000 rpm for 5 min at 4 °C. The aqueous extract of *Asparagus racemosus* leaf obtained in this manner was used as a capping and stabilizing agent during the synthesis of NiS NPs. In a typical synthesis of NiS NPs, leaf extract (10 ml) was added in to 50 ml nickel nitrate (5 mM) solution followed by addition of sodium sulfide (50 ml, 5 mM) under magnetic stirring. The content was later placed on a rotatory orbital shaker operating at 200 rpm, 30 °C for 12 hrs in dark condition. Particle formations were monitored by sampling an aliquot (3 ml) followed by measurement of the UV-vis spectra using spectrophotometer (Optizen 3220 UV, Korea). To find the absorption maximum or $\lambda_{max}$, a spectral scanning analysis was carried out by measuring optical density of the content from wavelength, 250 to 700 nm. Photoluminescence (PL) spectra were recorded in Varian (Cary Eclipse) spectrofluorimeter using 90° illumination. Initially, prescan was performed to find the excitation and emission maxima for the NiS nanoparticles. Excitation and emission slit widths were kept at 5 and 10.0 nm, respectively. Entire scanning was at the speed of 600 nm/min and data were analyzed using the WINFLR software.

### 2. TEM, SAED, XRD, EDAX and FT-IR

A thin film of the sample was prepared on a carbon coated copper grid and subjected to transmission electron microscopic (TEM, Techni 20, Philips, Holland) analysis. The aqueous solution of NiS was centrifuged at 13,000 rpm for 10 min. The recovered pellet was washed with 50 ml of 1 : 1, acetone in water solution for removal of organic impurities and centrifuged again at the same speed and for similar duration. Finally, pellet was freeze dried using a lyophilizer (Labconco, Missouri, USA). The elemental analysis of synthesized nanoparticles was determined by an electron microscope (Philips, Netherlands) equipped with energy dispersive X-ray spectroscopic system (EDAX-XL-30) operating at 15-25 KV and X-ray powder diffraction study. XRD data were collected using a Phillips PW1710 diffractometer with Cu-K$\alpha$ radiation operating at 40 kV, 35 mA in step scan mode, between 5 and 75° and with a counting time of 8 s per step. Disc of 100 mg KBr containing 1% freeze dried NiS containing powder served as material for recording transmission spectra. Spectral scan analysis was t at wave number ranging from 400-4,000 $cm^{-1}$ by using an FT-IR spectrometer (Perkin Elmer, Spectrum GX, USA) with resolution of 0.15 $cm^{-1}$ to evaluate functional groups of the *Asparagus racemosus* extract that might be involved in particle formation process.

### 3. Sorption of Dye on NiS Nanoparticles, Decolorization and LC-MS Study

Sorption experiments were at batch scale by adding different amount of synthesized NiS NPs in to 100 ml of malachite green solution. The flasks containing a mixture of sorbate and sorbent were placed onto a rotatory orbital shaker operating at 110 rpm until equilibrium time was reached. The solution of sorbate that did not contain NiS for sorption acted as a blank in this study. An aliquot of the sample was collected over an intermittent period of time followed by its filtration using 0.22 μm filter paper. The optimization for maximum sorption of malachite green was tested at contact time 5, 10, 15, 30, 45 and 60 min, sorbent concentration 0.25, 0.5, 1.0, 1.5, 2 g/L and sorbate concentration 25, 50, 75, 100 and 150 mg/L, respectively. The sorption of the dye was calculated by following equation:

$$\text{Sorption} = \frac{C_i - C_f}{C_i} \tag{1}$$

The sorption capacity was expressed as the amount of dye sorbed per gram of sorbent (mg/g) and calculated as follows:

$$q_e\left(\frac{mg}{g}\right) = \frac{(C_i - C_f)v}{M} \tag{2}$$

where $C_i$ and $C_f$ are the initial and final concentrations (mg/L) of dye in the aqueous solution, respectively. V is the volume (L) of test solution and M is the mass (g) of synthesized NiS, used as a sorbent. The degradation of dye (100 mg/L) dissolved in water (200 ml) was achieved by illuminating the solution with white light source. The dye solution and NiS nanoparticles (200 mg) in petri dish (150 mm) were illuminated with a table lamp fitted with 15 watt compact fluorescent light (CFL, 60 lumen/watt) bulb for 12 hrs. The spectral analysis of exposed dye solution was performed for determination of extent of photo bleaching activity by synthesised nanoparticles. The concentration of dye in solution was determined by examining its $\lambda_{max}$ at 621 nm. Degraded products of malachite green azo dye were analyzed by method adopted by Chen et al. [33] where HPLC-MS system (Thermo Scientific, LCQ Fleet™ Ion Trap Mass Spectrometer and Waters, USA) was used. Each sample, 25 μL, was filtered using filter assembly fitted with 0.22 μm pore size membrane filter prior to injection into an HPLC-MS system. A reverse phase, C18 HPLC column (150×2.1 mm, 5 μm particle size) was used for separation of degraded dye products. Gradient elution was performed using mobile phase (water and acetonitrile), while Analyst QS and Chem Draw software were used for prediction of the structure of degraded dye product based on deduced masses.

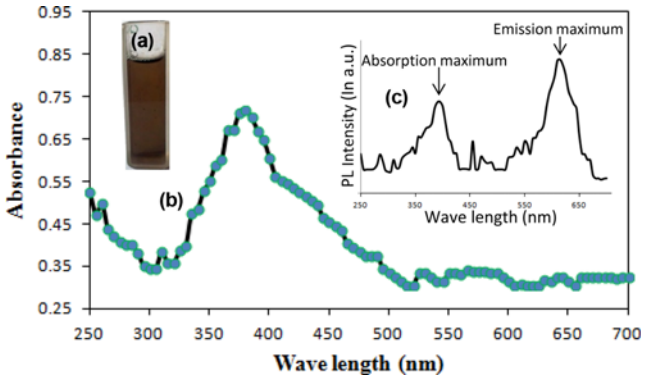


**Fig. 1. A visible observation of change in color during NiS nanoparticle formation. A cuvette containing 5 mM $Ni(NO_3)_2$ and *Asparagus racemosus* plant leaf extract after addition of 5 mM of $Na_2S$. A dark gray color appeared when mixture was incubated for 12 hrs (a). UV-vis spectra of colloidal NiS nanoparticles synthesized using plant leaf extract (b) at 12 hrs. Photoluminescence spectra of QDs nanoparticles synthesized using leaf extract (c).**

## RESULTS AND DISCUSSION

### 1. UV-vis Spectroscopy and Photoluminescence of NiS Nanoparticles

A colloidal solution of NiS nanoparticles was obtained by mixing the solution of $Ni(NO_3)_2$ in leaf extract and $Na_2S$. Initially, at 0 hr mixture was light green, which ultimately turned into dark grey color after 12 hrs (Fig. 1(a)). NiS nanoparticles displayed similar change in color in case of the study conducted by [34]. In control experiments where leaf extract was not added to $Ni(NO_3)_2$ solution, insoluble dark brown precipitates of NiS were observed. The absorption maximum of colloidal solution of NiS nanoparticles was found at 385 nm (Fig. 1(b)). Additionally, the optical properties of synthesized NiS nanoparticles were evaluated by recording photoluminescence spectra. Fig. 1(c) shows photoluminescence spectra of NiS nanoparticles synthesized by using leaf extract. The excitation peak was found at 385 nm, while an emission peak was observed at 615 nm. The excitation peak at 385 nm was very well correlated with absorption maxima recorded with UV-vis spectrophotometer (385 nm). Similar findings have been observed by Yang et al., where NiS nanocrystallite embedded in sol-gel silica xerogel was subjected to PL studies [35].

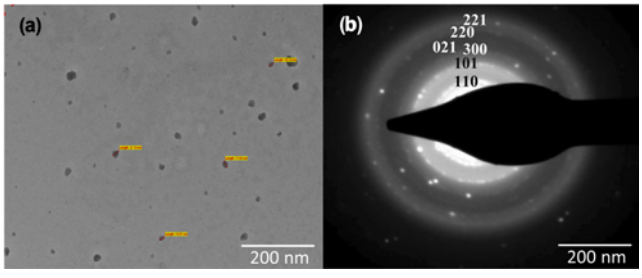


**Fig. 2. TEM micrographs recorded from drop-cast films of NiS nanoparticles solution (a). Selected area electron diffraction (SAED) pattern recorded from the NiS nanoparticles (b). The bar scale in photomicrograph shows 200 nm.**

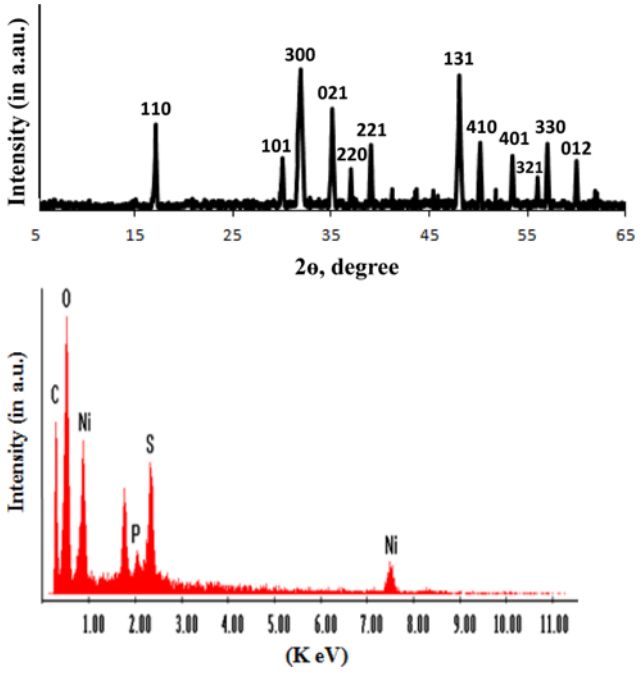


**Fig. 3. XRD diffractogram of NiS nanoparticles (a), EDAX pattern of synthesized NiS nanoparticles (b).**

### 2. TEM, EDAX, XRD and FT-IR Study

TEM analysis of stable colloidal solution indicated the formation of nearly spherical NiS nanoparticles. Formation of variable size of particles (~4-27 nm) suggested that the method adopted in this study produced polydispersed nanoparticles (Fig. 1(a)). Fig. 2(b) shows selected area electron diffraction (SAED) pattern of NiS nanoparticles. Results indicated that particles were crystalline as appearance of diffraction rings that corresponds to diffraction plane of 110, 101, 300, 021, 220 and 221, respectively, were obtained. The X-ray diffraction patterns obtained for NiS nanoparticles synthesized using leaf extract are shown in Fig. 3(a). The XRD diffractogram contained twelve prominent peaks that were clearly distinguishable. All of them can be perfectly indexed to hexagonal crystalline NiS not only in peak position, but also in their relative intensity. The peaks with $2\theta$ values of 17.23, 29.94, 32.15, 35.63, 37.1, 39.11, 48.21, 51.64, 53.33, 55.04, 57 and 59.98 corresponded to the crystal planes of 110, 101, 300,021, 220, 221, 131, 410, 401, 321, 330 and 012 plane of crystalline NiS, respectively. The XRD diffractogram matched the standard diffraction (JCPDS, file No.-12-0041) pattern of NiS. EDAX analysis gives qualitative as well as quantitative status of elements that may be involved in formation of nanoparticles. Fig. 3(b) shows the elemental profile of synthesized nanoparticles. The analysis revealed that apart from Ni (32.17%) and S (30.89%), elements like O (14.05%), C (12.24%), and P (9.32%) were integral parts of synthesized NiS. FT-IR analysis identified the interaction among biomolecules of the leaf extract and metal ions, responsible for formation and stabilization of NiS nanoparticles. Fig. 4(a) shows the absorption spectrum of the sample that did not contain metal sulfide, while Fig. 4(b) shows the spectrum of the sample that contained NiS. Spectra 4(a) showed absorption peaks at 3441,

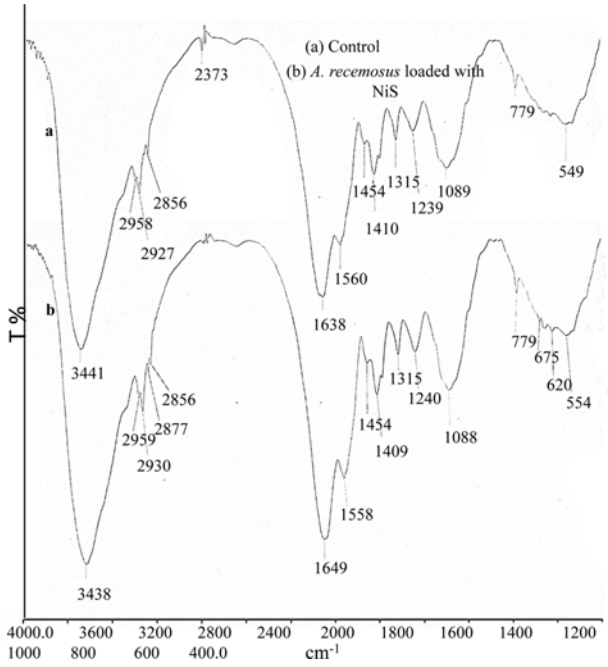


**Fig. 4. FT-IR spectra of NiS treated *Asparagus racemosus* extract: (b), and untreated extract: (a).**

2,958, 2,927, 2,856, 2,373, 1,638, 1,560, 1,454, 1,410, 1,315, 1,239, 1,089, 779 and 549 $cm^{-1}$, respectively. Similarly, the absorption peaks of the sample (Fig. 4(b)) that contained NiS were obtained at 3,448, 2,959, 2,930, 2,877, 2,856, 1,649, 1,558, 1,454, 1,409, 1,315, 1,240, 1,088, 779, 675, 620 and 544 $cm^{-1}$, respectively. The absorption peak at 3,441 was shifted at 3,448; similarly, the peak at 2,927 was shifted at 2,930, and an additional peak at 2,877 was obtained. Peak at 2,373 (in control) was found to absent in the sample. Peaks at 1,638 and 1,560 were shifted to 1,649 and 1,558, respectively. In fingerprint region the absorption peaks from 1,454 to 779 remained unaltered. However, absorption peaks at 675, 620 and 544 in the sample were identified. Shift in absorption peaks 3,441 to 3,448 indicated the involvement of N-H group, while the appearance of a peak at 2,877 and reduction of peak height at 2,373 suggested the involvement of O-H group [36]. Peaks between two wave numbers 2,300-2,100 $cm^{-1}$ can be assigned to presence and involvement of triple bond molecules in organic mixture. There was no visible sign of peaks between these wave numbers, suggesting that phytochemicals present in the leaf extract may have contained very small amount of molecules containing C≡C alkynes and C≡N nitriles. Shift of peak from 1,638 to 1,649 indicated the involvement of a group of double bond hetero atoms like C=O, C=C and C=N. Peaks between finger print region, i.e., 1,500-400 $cm^{-1}$ are due to all manner of bending vibrations within the molecules. The peaks around 1,300 and 1,200 are attributed to the stretching vibration of single bond between C-O. The peaks around 1,200 and 1,000 may be due to stretching and vibration between N-H. Shift in absorption from 1,239 to 1,240 that occurred due to vibrations in bond between N-H element. Absorption peaks at 675 and 620 $cm^{-1}$ in the sample may be due to the partial deutriation of amine or carboxyl group.

### 3. Effect of Contact Time and Adsorbent Doses on Adsorption

Effect of contact time on sorption of MG onto NiS NPs was studied using sorbent doses 1 g/L and sorbate 100 mg/L at 30 °C. Sorption of MG (0.26 mM) was observed after mixing sorbate and sorbent for 30 min (Fig. 5(a)). Fig. 5(b) shows the pattern for absorption of MG at different dose of sorbent. Data indicated equilibrium in sorption of analyte upon increase in NiS NPs loading beyond

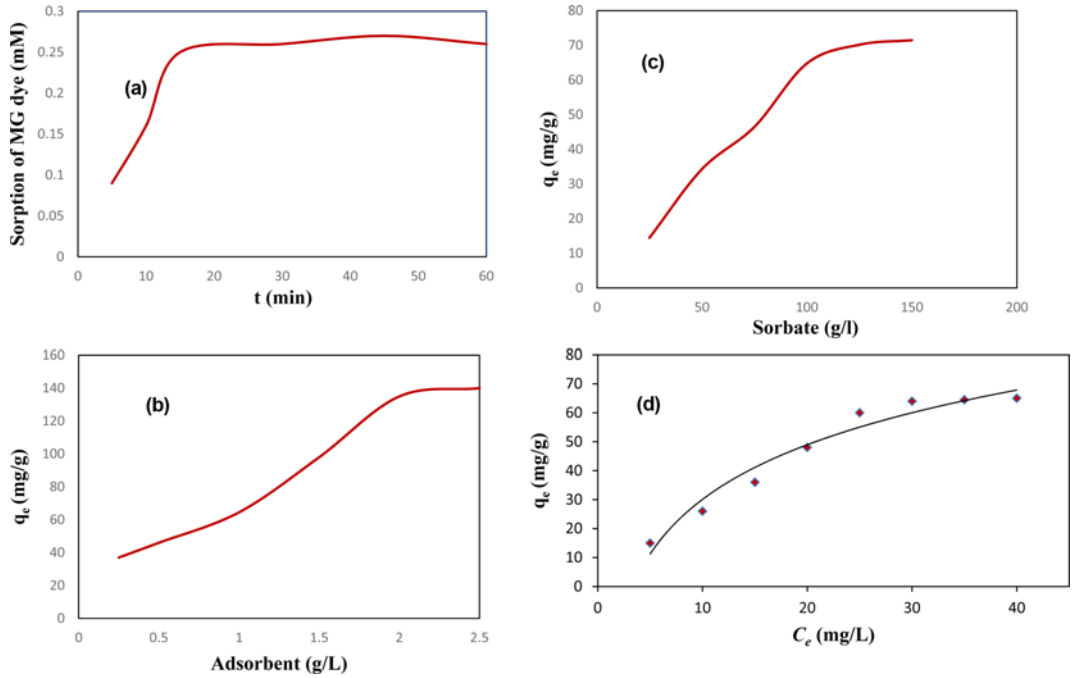


**Fig. 5. Effect of contact time (a) on sorption of MG onto sorbent (dye concentration: 0.275 mM, sorbate concentration: 2 g/L at 30 °C). Effect of sorbent, (b) and effect of sorbate (c) on over all sorption processes. Freundlich isotherm plots for sorption of MG onto sorbent (d).**

1 g/L. Maximum sorption occurred when 1 g/L of the NiS was subjected to sorption studies. Similarly, an increase in analyte concentration to more than 100 mg/L, when sorbent dose was 1 g/L, did not enhance overall sorption in batch sorption model (Fig. 5(c)).

**4. Adsorption Isotherms**

The sorption isotherms were investigated using three equilibrium models: Langmuir, Freundlich and Dubinin-Radushkevich (D-R) isotherm models. The Langmuir model assumes that the uptake of dye on to a solid is a monolayer adsorption process, without any interaction between sorbed dye molecules. Langmuir isotherm can be defined according to the following formula:

$$q_e = \frac{q_m K_L C_e}{1 + K_L C_e} \quad (3)$$

where $q_e$ is the equilibrium dye concentration on the adsorbent (mg/g), $C_e$ is the equilibrium dye concentration in the solution (mg/L), $q_m$ is the monolayer sorption capacity of the adsorbent (mg/g) and $K_L$ is the Langmuir sorption constant (L/mg), relating the free energy of sorption. The coefficients of determination ($R^2$) were found to be 0.9568 for the MG dye sorption. The maximum sorption capacity ($q_m$) of the sorbent was found to be 64.85 mg/g for the dye molecules. The $K_L$ value was calculated as 0.026 L/mg for the dye sorption. The Freundlich model assumes a heterogeneous adsorption surface and active sites with different energy. This isotherm can be explained by following formula:

$$q_e = K_f C_e^{1/n} \quad (4)$$

where $K_f$ is a constant relating the sorption capacity and 1/n is an empirical parameter related to sorption intensity which varies with the heterogeneity of the material. The Freundlich isotherm was obtained by plotting $q_e$ Vs. $C_e$ values, which showed a nonlinear relationship between two (Fig. 5(d)). Values of $K_f$ and 1/n were found to be 3.35 and 0.54 for MG sorption. The 1/n values, between 0 and 1 indicated that the adsorption of dye onto the sorbent was favorable at studied conditions with $R^2$ value 0.9311 for MG sorption. These results suggested that the Freundlich model was not able to describe the relationship between the amounts of sorbed dye adequately to their equilibrium concentration in the solution. The Langmuir isotherm model best fitted the equilibrium data since it presented higher $R^2$ value than did the Freundlich model. Physical or chemical nature of sorption processes was studied by analyzing the equilibrium data using D-R isotherm model. The linear form of D-R isotherm model is presented by following equation:

$$\ln q_e = \ln q_m - \beta\varepsilon^2 \quad (5)$$

where $q_e$ is the amount of dye adsorbed on per unit weight of NiS NPs (mg/g), $q_m$ is the maximum sorption capacity (mg/g), $\beta$ is the activity coefficient related to mean sorption energy ($mol^2/J^2$) and $\varepsilon$ is the Polanyi potential $\varepsilon = RT \ln(1+1/C_e)$. The D-R isotherm model well fitted the equilibrium data since the $R^2$ value was found to be 0.9963 for MG dye (Fig. 6(a)). The $q_m$ value was found by using the intercept of the plots as $0.649\times10^2$ mg/g for the dye. The sorption mean free energy (E; kJ/mol) gives information about nature of adsorption, i.e., physical or chemical. The mean sorption energy (E; kJ/mol) is expressed as follows:

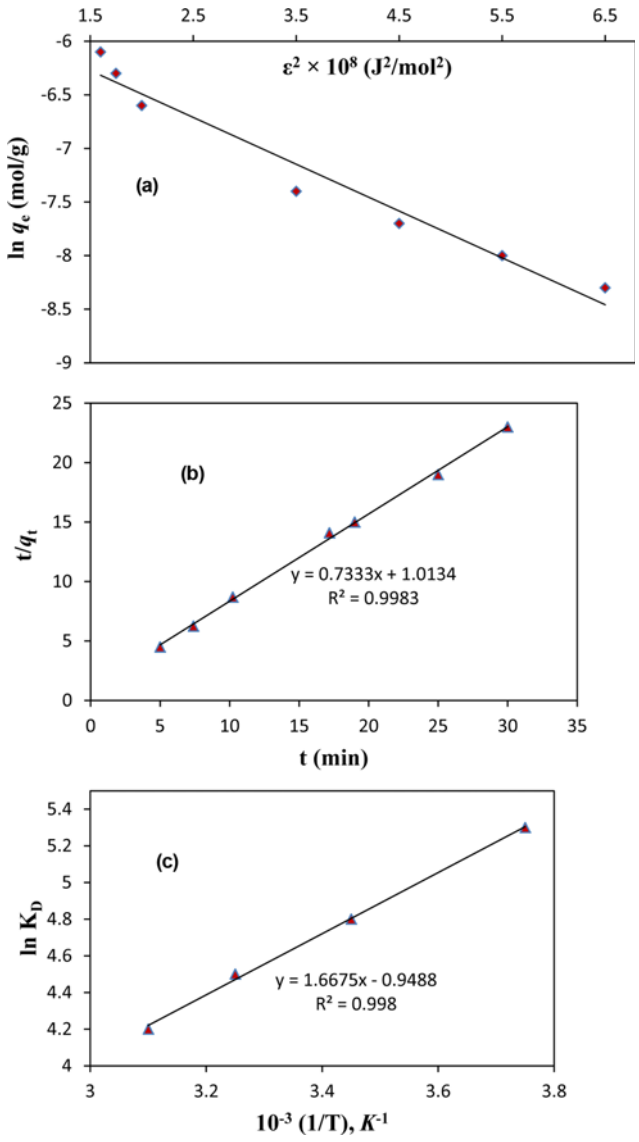


**Fig. 6. D-R isotherm plots for sorption of MG (a). Sorption kinetic models for dye uptake (b) Plot of ln $K_D$ Vs. 1/T for the estimation of thermodynamic parameters for dye molecules (c).**

$$E = \frac{1}{\sqrt{2\beta}} \quad (6)$$

The adsorption process is regarded as chemical when values lie between 8 and 16 kJ/mol; similarly, adsorption is physical when E value is less than 8 kJ/mol. The mean sorption energy was calculated as 5.73 kJ/mol for sorption of MG dye. The dye sorbed physically onto sorbent, since the sorption energy was found to be less than 8 kJ/mol.

**5. Adsorption Kinetic Models**

To evaluate sorption dynamics, kinetic constants can be used to optimize the residence time of a biosorption process. Pseudo-first order and Pseudo-second order kinetic models were used to analyze the sorption rate of MG on NiS NPs. The pseudo-first order rate equation is given as;

$$\log(q_e - q_t) = \frac{\log q_e - k_t t}{2.303} \quad (7)$$

where $q_e$ (mg/g) is the amount of metal ions sorbed at equilibrium and $q_t$ is the amount of metal sorbed at any time (mg/g) and $k_1$ is the rate constant of the equation ($min^{-1}$). The biosorption rate constant $k_1$ can be can be determined experimentally by plotting, log ($q_e$–$q_t$) versus t. Experimental data were also tested by pseudo-second-order [37] equation

$$\frac{t}{q_t} = \frac{1}{k_2 q_e^2} + \left(\frac{1}{q_e}\right)t \quad (8)$$

where $k_2$ is the equilibrium rate constant (g/mg/min). The value of the correlation coefficient of pseudo-second order model (Fig. 6(b)) was found to be 0.9914 for MG dye, which is higher than pseudo-first-order model: 0.8944. Compared to the pseudo-first order equation, the pseudo-second order model can explain the biosorption kinetic behavior of MG onto sorbent satisfactorily with a good correlation coefficient.

**6. Sorption Thermodynamics and Kinetic Studies**

Thermodynamic behavior of the adsorption of dye onto sorbent including the change in free energy ($\Delta G^o$), enthalpy ($\Delta H^o$) and entropy ($\Delta S^o$) has been studied. The change in free energy ($\Delta G^o$) was calculated from the following equation:

$$\Delta G^o = -RT \ln K_D \quad (9)$$

where, R is the universal gas constant (8.314 J/mol K), T is temperature (K) and $K_D$ ($q_e/C_e$) is the distribution coefficient. The enthalpy ($\Delta H^o$) and entropy ($\Delta S^o$) parameters were estimated from the the following equation:

$$\ln K_D = \left(\frac{\Delta S^o}{T}\right) - \left(\frac{\Delta H^o}{RT}\right) \quad (10)$$

The $\Delta H^o$ and $\Delta S^o$ were calculated from the slope and intercept of the plot of ln $K_D$ versus 1/T yields and shown in Fig. 6(c). Gibbs free energy change ($\Delta G^o$) was found to be −18.64, −18.59, −17.66 and −17.02 kJ/mol for MG adsorption at 20, 30, 40 and 50 °C, respectively. The negative $\Delta G^o$ values indicated thermodynamically feasible and spontaneous nature of the sorption. The decrease in $\Delta G^o$ values with increase in temperature suggested the lesser feasibility of sorption at high temperatures. The enthalpy of sorption $\Delta H^o$ parameter was found to be −5.32 kJ/mol for dye sorption. The negative $\Delta H^o$ indicates the exothermic nature of sorption. The enthalpy or the heat of sorption ranging from 2.1 to 20.9 KJ/mol corresponds to physical sorption, whereas ranging from 20.9 to 418 KJ/mol is regarded as chemical sorption. Therefore, the $\Delta H^o$ value suggests that the sorption process of MG onto sorbent occurred due to physical sorption. The $\Delta S^o$ parameter was found to be −12.56 J/mol K for dye sorption. The negative $\Delta S^o$ value suggested a decrease in the randomness at the solid/solution interface during the sorption process. Photocatalytic experiments on degradation of aqueous MG by NiS NPs were conducted in batch mode to assess the particles' ability to degrade the dye under white light illumination. The pH of solution was kept constant during the experiment at ~7. The initial temperature of the solution was 30 °C. Since exposure to MG by white light was conducted for 12 h, we assumed that during this

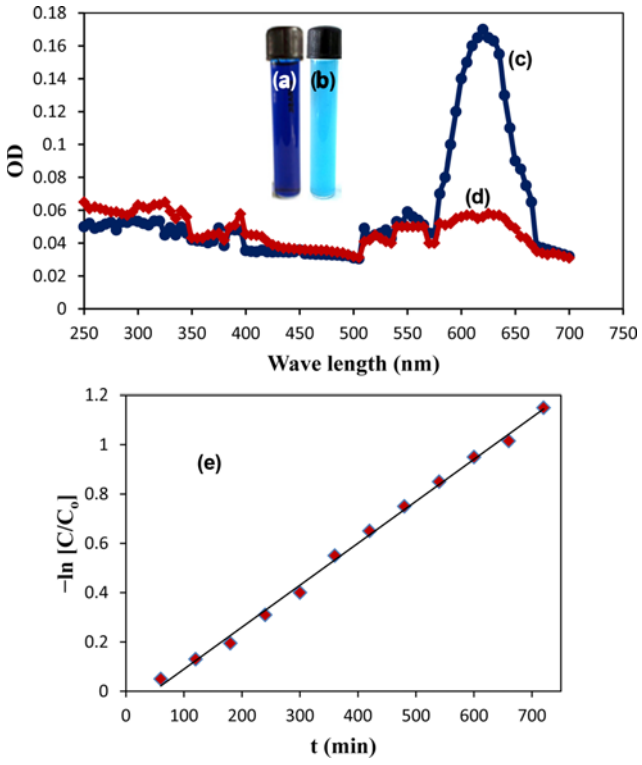


**Fig. 7. Photograph of MG dye, in absence of NiS NPs and before illumination to white light source (a) and after illumination, in presence of nano NiS (b). UV-vis absorption pattern of control MG dye (c) as well as after exposure (d). Degradation kinetics of MG dye by NiS NPs (e).**

period all the dissolved dye molecules were in contact with NiS nanoparticles. The exposed dye solution was found to be decolorized (Fig. 7(a) and (b)). This change in color indicated a sign of degradation of the dye molecule. To examine the absorption pattern of the original dye solution as well as decolorized dye present in degraded sample, UV-vis scanning procedure was carried out. There was a significant reduction in absorption maximum at 620 nm in comparison to control dye solution (Fig. 7(c) and (d)). The MG degradation kinetics data were examined using a first-order kinetic expression:

$$\text{rate} = -\frac{dc}{dt} = -Kc \quad (11)$$

$$\ln\left[\frac{Co}{C}\right] = -Kt \quad (12)$$

where C is the conc. of MG at time t, Co is the initial conc. of the dye, K is the first-order rate constant and t is time. The first-order rate constant K is obtained by plotting ln[Co/C] vs time (min). The corresponding first-order degradation rate constant was found to be 0.018 $min^{-1}$ (Fig. 7(e)).

**7. MG Intermediates Identification**

The presence of intermediates of MG in decolorized sample was anticipated, as an abrupt change in absorption pattern of light spectrum was obtained. The filtrate of decolorized as well as control sample was examined by LC-MS analysis, which suggested the cleav-

age of bonds in dye molecules. During liquid chromatography of the control sample, a prominent peak corresponding to retention time of C18 column was obtained at 19.45 min. The mass spectra (m/z) value of this compound was found to be 358.05. The decolorized product of MG yielded LC peaks at 2.79, 3.31 and 9.48 min. The MS analysis of the peak at 2.79 min yielded m/z value, 76.58; similarly, peaks at 3.31 and 9.48 min yielded m/z value of 105.75 and 135.43. The mass value suggested the presence of benzene, benzaldehyde and dimethyl aminophenol as intermediate product in decolorized sample (supplementary Fig. 1).

## CONCLUSIONS

Colloidal solution of NiS nanoparticles was obtained by using leaf extract of plant *Asparagus racemosus*. Results indicated the formation of nearly spherical nanoparticles of radius ranging from 4-27 nm. The maximum sorption capacity of NiS nanoparticles for MG dye was 64.85 mg/g. Sorbed dye illuminated with light resulted in the cleavage of bonds of parent dye molecules into relatively smaller molecules. LC-MS analysis of decolorized dye sample indicated the presence of benzene, benzaldehyde and dimethyl aminophenol in aqueous solution. Integration of NiS nanoparticles application in primary waste water treatment process can be a promising step where they catalytically decompose the original structure of dye molecules.

## ACKNOWLEDGEMENT

KSP is grateful to Mr. Vipul J. Patel, senior scientific officer at DST (Department of Science and Technology, India) sponsored SICART (Sophisticated Instrumentation Centre for Applied Research and Testing, Anand, Gujarat, India) for his help in analysis of samples.

## REFERENCES

1. S. J. Allen, G. McKay and J. F. Porter, *J. Colloid Interface Sci.*, **280**, 322 (2004).
2. R. Jaskot, *Fundam. Appl. Toxicol.*, **22**, 103 (1994).
3. A. Dipple, C. Anita and H. Bigger, *Mutat. Res. Toxicol.*, **259**, 263 (1991).
4. S. Bilgi and C. Demir, *Dye. Pigm.*, **66**, 69 (2005).
5. R. Molinari, F. Pirillo, M. Falco, V. Loddo and L. Palmisano, *Chem. Eng. Process. Process Intensif.*, **43**, 1103 (2004).
6. E. Forgacs, T. Cserháti and G. Oros, *Environ. Int.*, **30**, 953 (2004).
7. L. Zhu, Z. D. Meng, T. Ghosh and W. C. Oh, *J. Korean Ceram. Soc.*, **49**, 135 (2012).
8. E. Franciscon, M. J. Grossman, J. A. R. Paschoal, F. G. R. Reyes and L. R. Durrant, *Springerplus.*, **1**, 37 (2012).
9. C. J. Cha, D. R. Doerge and C. E. Cerniglia, *Appl. Environ. Microbiol.*, **67**, 4358 (2001).
10. C. R. Nelson and R. A. Hites, *Environ. Sci. Technol.*, **14**, 1147 (1980).
11. M. Banerjee, L. Chongad and A. Sharma, *Res. J. Recent Sci.*, **2**, 326 (2013).
12. R. Comparelli, F. Zezza, M. Striccoli, M. L. Curri, R. Tommasi and A. Agostiano, *Mater. Sci. Eng. C.*, **23**, 1083 (2003).
13. S. G. Patel, S. Bhatnagar, J. Vardia and S. C. Ameta, *Desalination*, **189**, 287 (2006).
14. A. Sharma, S. Rastogi and M. Sindal, *Int. J. Chem. Sci.*, **9**, 1569 (2011).
15. H. Guo, Y. Ke, D. Wang, K. Lin, R. Shen, J. Chen and W. Weng, *J. Nanoparticle Res.*, **15**, 1475 (2013).
16. A. Nezamzadeh-Ejhieh and M. Khorsandi, *Iran. J. Catal.*, **1**, 99 (2011).
17. A. Nezamzadeh-Ejhieh and M. Khorsandi, *J. Hazard. Mater.*, **176**, 629 (2010).
18. V. Sharma, N. Gandhi, A. Khant and R. C. Khandelwal, *Int. J. Chem. Sci.*, **8**, 1965 (2010).
19. A. D. Bokare, R. C. Chikate, C. V. Rode and K. M. Paknikar, *Appl. Catal. B Environ.*, **79**, 270 (2008).
20. R. Comparelli, E. Fanizza, M. L. Curri, P. D. Cozzoli, G. Mascolo and A. Agostiano, *Appl. Catal. B Environ.*, **60**, 1 (2005).
21. J. W. Yoon, M. H. Baek, J. S. Hong, C. Y. Lee and J. K. Suh, *Korean J. Chem. Eng.*, **29**, 1722 (2012).
22. B. Thongrom, P. Amornpitoksuk, S. Suwanboon and J. Baltrusaitis, *Korean J. Chem. Eng.*, **31**, 587 (2014).
23. L. Cao, J. Zhang, S. Ren and S. Huang, *Appl. Phys. Lett.*, **80**, 4300 (2002).
24. B. Tryba, A. W. Morawski and M. Inagaki, *Appl. Catal. B Environ.*, **41**, 427 (2003).
25. L. Qi, H. Cölfen and M. Antonietti, *Nano Lett.*, **1**, 61 (2001).
26. S. K. Haram, B. M. Quinn and A. J. Bard, *J. Am. Chem. Soc.*, **123**, 8860 (2001).
27. J. Zhang, Y. Wang, J. Zheng, F. Huang, D. Chen, Y. Lan, G. Ren, Z. Lin and C. Wang, *J. Phys. Chem. B.*, **111**, 1449 (2007).
28. L. M. Liz-Marzán and I. Lado-Touriño, *Langmuir*, **12**, 3585 (1996).
29. M. P. Pileni, *Pure Appl. Chem.*, **72**, 53 (2000).
30. K. S. Prasad, Y. Amin and K. Selvaraj, *J. Hazard. Mater.*, **276**, 232 (2014).
31. K. S. Prasad and K. Selvaraj, *Biol. Trace Elem. Res.*, **157**, 275 (2014).
32. K. S. Prasad, H. Patel, T. Patel, K. Patel and K. Selvaraj, *Colloids Surf. B. Biointerfaces*, **103**, 261 (2013).
33. C. C. Chen, C. S. Lu, Y. C. Chung and J. L. Jan, *J. Hazard. Mater.*, **141**, 520 (2007).
34. L. Wang, M. Schultz and E. Matijević, *Colloid Polym. Sci.*, **275**, 593 (1997).
35. P. Yang, M. Lu, C. F. Song, G. Zhou, D. Xu and D. R. Yuan, *J. Phys. Chem. Solids.*, **63**, 2047 (2002).
36. K. S. Prasad, T. Amin, S. Katuwa, M. Kumari and K. Selvaraj, *Arab. J. Chem.* (2014), DOI:10.1016/j.arabjc.2014.05.033.
37. Y. Ho and G. McKay, *Process Biochem.*, **34**, 451 (1999).